

Article

Clustering of Asphalt Pavement Maintenance Sections Based on 3D Ground-Penetrating Radar and Principal Component Techniques

Huimin Liu ¹, Jianhao Zheng ², Jiangmiao Yu ^{3,4,*}, Chunlong Xiong ^{3,5,*} , Weixiong Li ⁵ and Jie Deng ⁶¹ Guangdong Highway Construction Co., Ltd., Guangzhou 510100, China; liuhm@gdhighway.com.cn² Guangdong Provincial Freeway Co., Ltd., Guangzhou 510100, China³ School of Civil Engineering and Transportation, South China University of Technology, Guangzhou 510640, China⁴ State Key Laboratory of Subtropical Building and Urban Science, Guangzhou 510641, China⁵ Guangzhou Xiaoning Roadway Engineering Technology Research Institute Co., Ltd., Guangzhou 510641, China⁶ Guangdong Boda Expressway Co., Ltd., Boshen Branch, Guangzhou 510641, China; dengjie@gdhighway.com.cn

* Correspondence: yujm@scut.edu.cn (J.Y.); cthgclx@mail.scut.edu.cn (C.X.)

Abstract: Asphalt pavement maintenance section classification is an important prerequisite for accurately determining asphalt pavement maintenance needs and formulating accurate maintenance plans. This paper introduces the three-dimensional (3D) ground-penetrating radar (GPR) pavement internal crack rate index on the basis of an original road surface performance data matrix, and the dimensionality of the road section classification data matrix was reduced through the principal component technique. An analysis of variance was used to compare the significance of the differences in the results for road section classification using different clustering methods and different clustering data and to investigate the influence of the clustering method, principal component technique and crack rate index on the maintenance road section classification results. The results showed that the principal component technique could reduce the dimensionality of the data matrix by 33% and retain more than 84% of the information. There was a genetic relationship between the clustering data and the technical characteristics of the classified sub-sections, and the internal crack rate was important for the characterisation of internal defects in asphalt pavement sub-sections and the determination of maintenance needs. The results of section classification varied considerably between clustering methods, and the choice of clustering method had a relationship to the pavement maintenance objectives. The dynamic clustering method combined with principal component analysis could significantly improve the significance of the differences in the clustering results, effectively improving the division of maintenance sections.

Keywords: 3D GPR; principal components; internal crack rate; clustering; analysis of variance

Citation: Liu, H.; Zheng, J.; Yu, J.; Xiong, C.; Li, W.; Deng, J. Clustering of Asphalt Pavement Maintenance Sections Based on 3D Ground-Penetrating Radar and Principal Component Techniques. *Buildings* **2023**, *13*, 1752. <https://doi.org/10.3390/buildings13071752>

Academic Editor: Ramadhansyah Putra Jaya

Received: 26 June 2023

Revised: 6 July 2023

Accepted: 7 July 2023

Published: 10 July 2023



Copyright: © 2023 by the authors. Licensee MDPI, Basel, Switzerland. This article is an open access article distributed under the terms and conditions of the Creative Commons Attribution (CC BY) license (<https://creativecommons.org/licenses/by/4.0/>).

1. Introduction

1.1. Background

Maximising technical and economic benefits is the ultimate goal of scientific decision making for preventive maintenance [1,2]. The scientific decision, which is mainly about applying the right preventive maintenance measures in the right place at the right time, usually includes the determination of the maintenance timing, the division of maintenance intervals and the selection of maintenance solutions [3,4]. Segmenting is an important technical tool to differentiate the maintenance needs of different segments and to allocate maintenance resources appropriately [5–7].

The initial division of asphalt pavement preventive maintenance sections is usually based on geology, weather, traffic, bridging, culverting, tunnel structure distribution and other spatial characteristics, with the same external condition characteristics of the various

components of the road section being pre-divided into categories [8–10]. This method is still used in current maintenance management practice due to its simplicity of operation, but the results of section classification are fixed. It is difficult to relate this classification to the variability of external conditions, pavement disease characteristics (especially internal pavement disease characteristics), etc. With the development of preventive maintenance techniques [11,12], scholars have undertaken more in-depth research on the classification of maintenance sections, and the importance of asphalt pavement distress characteristics in section classification has increased [13–15]. The development of more efficient classification algorithms has become a major research hotspot, aiming to help fully exploit the differentiated information for asphalt pavement sections [16–18].

The above research has greatly contributed to the advancement of scientific decision making in preventive maintenance plans but still remains at the level of using surface functional indicators as the basis. These studies have limitations because internal pavement distress is easily covered by frequent preventive maintenance and surface indicators do not fully reflect the whole pavement condition [19,20]. Although methods for determining the preventive or structural maintenance needs of different road sections have been proposed [21,22], in practice, it is often found that several road sections that have been determined to be in need of preventive maintenance require preventive maintenance of different intensity or with different capacity levels because of the differences in the internal condition of these sections. Unfortunately, the technical indicators on which decision making about asphalt pavement maintenance plans is based do not so far include indicators of pavement internal damage, such as cracks, and relevant studies are less common [8,23–25].

When a certain clustering algorithm is used for a certain set of clustered data, the optimal classification result can be obtained from the iteration of the algorithm, but the samples under different classes do not necessarily have statistically significant differences, and it is difficult to match the pavement maintenance decision-making plan with the actual demand. This problem reduces the reliability of the classification results for asphalt pavement maintenance sections. Unfortunately, while previous studies have focused on the improvement of specific algorithms' own classification effects, there is a lack of in-depth research on the composition of clustering data, the choice of clustering methods and the relationship between them [26–28].

1.2. Objective and Scope

The objectives of this study were first to adopt the three-dimensional GPR-based pavement internal crack rate index and the principal component technique to realize the segmentation of asphalt pavement maintenance sections and secondly to analyse the influence of different clustering methods and clustering data on the classification results. This will provide a theoretical basis for the determination of the basic data indicators and the selection of clustering methods for the classification of asphalt pavement and enable a more scientific classification of maintenance sections.

2. Methods

Cluster analysis is a method of classifying research objects without knowing how many classes they should be divided into using the help of statistical methods and based on the information already collected. The method of clustering analysis is to find some statistical quantities that objectively reflect the relationship between the research objects and their proximity. There are three main methods of cluster analysis: systematic clustering, dynamic clustering and ordered clustering [29,30].

2.1. Systematic Clustering Methods

The systematic clustering method, also named the hierarchical clustering method [31,32], is one of the most widely used all around the world. It involves first looking at the clustered samples or variables as specific groups, determining the similarity statistics between classes, selecting the two closest classes or a number of classes to merge

into a new class, calculating the similarity statistics between the new class and the other classes, and then selecting the two closest clusters or a number of clusters to merge into a new class until all the samples or variables are combined into one class. The specific steps for classifying road sections using the systematic clustering method are as follows:

Step 1: The project is pre-divided into n unit sections according to a fixed length l_0 . For each unit section, a sample set of m disease indicators is collected to form the sample set $X(n \times m)$ for the maintenance project, as shown by Equation (1):

$$X = \{x_{ij}\} = \begin{bmatrix} x_{11} & \cdots & x_{1m} \\ \vdots & \ddots & \vdots \\ x_{n1} & \cdots & x_{nm} \end{bmatrix}, (i = 1, 2, \dots, n; j = 1, 2, \dots, m) \quad (1)$$

where x_{ij} is the m th disease characteristic indicator in the n th unit section.

Due to the variation in the range of values for each disease characteristic indicator, x_{ij} is dimensionless for mathematical purposes, as shown by Equation (2):

$$x_{ij}^* = \frac{x_{ij} - \bar{x}_j}{s_j}, (i = 1, 2, \dots, n; j = 1, 2, \dots, m) \quad (2)$$

where \bar{x}_j is the mean of each characteristic variable, and s_j is the standard deviation.

The dimensionless sample set X^* is calculated according to Equation (3):

$$X^* = \begin{bmatrix} x_{11}^* & \cdots & x_{1m}^* \\ \vdots & \ddots & \vdots \\ x_{n1}^* & \cdots & x_{nm}^* \end{bmatrix} \quad (3)$$

Step 2: The distance d_{ij} between two sections of the n th unit is calculated.

Defining each of the n unit sections as a class, the number of classes for all the unit sections is $l = n$, and the matrix Y of sections of the conservation project is shown in Equation (4):

$$Y = \{X_i^*\}, (i = 1, 2, \dots, n) \quad (4)$$

The distance $d_{ii'}$ between two sections of the n th unit can be calculated using Equation (5):

$$d_{ii'} = \frac{1}{m} \sum_{j=1}^m |x_{ij}^* - x_{i'j}^*|, (i, i' = 1, 2, \dots, n) \quad (5)$$

Step 3: The two closest classes in the matrix Y are merged into one new class, and the number of classes in all unit sections of the combined project becomes $l = n - 1$. Then, in the new class, it is necessary to continue to find the two closest classes to merge and to repeatedly merge them until the classification ends when the number of divided sections reaches the target $l = t$. When a new class contains at least two unit sections, the distance between the classes is calculated according to Equation (6):

$$d_{RS} = \sqrt{\frac{1}{n_R n_S} \sum_{i \in Y_R, i' \in Y_S} d_{ii'}^2}, (n_R \geq 1, n_S \geq 1) \quad (6)$$

where d_{RS} is the distance between two new classes, Y_R and Y_S ; and n_R and n_S are the number of unit sections contained in them, respectively.

2.2. Dynamic Clustering Methods

The dynamic clustering method involves randomly selecting a group of coalescence points, letting the other samples coalesce towards the coalescence points according to some principle (usually the minimal Euclidean distance) and iterating on the coalescence points until the coalescence points are stable. A popular dynamic clustering method is the k-means method [33,34].

The specific steps for classifying road sections using dynamic clustering are as follows:

Step 1: The dimensionless processing of the raw data matrix is consistent with the systematic clustering approach;

Step 2: The number of categories t is specified and a random sample of X^* is selected as the cluster centre δ_c for each category.

$$\delta_c = (\delta_{c_1}, \delta_{c_2}, \dots, \delta_{c_t}) \tag{7}$$

$$\delta_{c_k} = (x_{\zeta_k 1}^*, x_{\zeta_k 2}^*, \dots, x_{\zeta_k m}^*), (k = 1, 2, \dots, t; \zeta_k = \text{index}(X_i^*, \text{randbetween}(1, n))) \tag{8}$$

where ζ_k is the serial number of the randomly selected sample in X^* ;

Step 3: The distance of each sample in X^* from each cluster centre δ_{c_k} is calculated.

$$d_{ic_k} = \sqrt{\sum_{j=1}^m (x_{ij}^* - \delta_{c_k j})^2}, (i = 1, 2, \dots, n; k = 1, 2, \dots, t) \tag{9}$$

Step 4: All samples with the smallest distance from δ_{c_k} in X^* are combined into one set (the set t can be obtained), and the updated cluster centres for each set are recalculated. The cluster centres are determined using an iterative calculation, and the cluster centres obtained in the η th iteration are denoted as $\delta_{c_k}^{(\eta)}$.

$$\delta_{c_k}^{(\eta)} = \frac{1}{N_k} \sum_{i=1}^{N_k} x_{ij}^*, (j = 1, 2, \dots, m; k = 1, 2, \dots, t) \tag{10}$$

where N_k is the number of samples in the new set k ;

Step 5: The final clustering result is obtained when the samples in the set corresponding to the update of the clustering centre $\delta_{c_k}^{(\eta+1)}$ for the step $\eta + 1$ match the samples in the set corresponding to the η th step clustering centre $\delta_{c_k}^{(\eta)}$.

2.3. Ordered Clustering Methods

Compared to systematic clustering methods in terms of sample data capacity, dynamic clustering methods have a greater range of application. However, both the methods disrupt the original unit sections denoted by asphalt pavement serial numbers; for example, the unit sections numbered 1, 3, 5 and 7 are classified as the first category, while the unit sections numbered 2, 4, 6 and 8 are classified as the second category. The two types of maintenance needs are different and require different maintenance programs. They must be constructed in phases, which greatly increases the difficulty of implementing maintenance construction, especially for projects with high traffic volumes, as well as increasing the frequency and reducing the efficiency of the deployment of construction equipment and other resources. Ordered clustering methods, also called optimal partitioning methods, can achieve a constant front-to-back order for each unit section [35,36]. The specific steps of the ordered clustering method are as follows:

Step 1: The dimensionless processing of the raw data matrix is consistent with the systematic clustering approach;

Step 2: The number of categories t is specified. It is assumed that one of the category is $C_{i'}$, which is listed in Equation (11):

$$C_{i'} = \{x_i^*, x_{i+1}^*, \dots, x_{i'}^*\}, (i' > i) \tag{11}$$

The mean value of $C_{i'}$ is calculated using Equation (12):

$$\bar{x}_{i'} = \frac{1}{i' - i + 1} \sum_{\zeta=i}^{i'} x_{\zeta}^* \tag{12}$$

The diameter $D_{i'}$ of each category of $C_{i'}$ is calculated using Equation (13):

$$D_{i'} = \sum_{\zeta=i}^{i'} (x_{\zeta}^* - \bar{x}_{i'})' (x_{\zeta}^* - \bar{x}_{i'}) \quad (13)$$

Step 3: The objective function is calculated.

A particular classification scheme is $C(n, t) : \{i', i + 1, \dots, i_2 - 1\}, \{i_2, i_2 + 1, \dots, i_3 - 1\}, \dots, \{i_t, i_t + 1, \dots, n\}$; then, the objective function is as shown by Equation (14):

$$e[C(n, t)] = \sum_{k=1}^{t-1} D(i_k, i_{k+1} - 1) \quad (14)$$

When n and t are fixed, the smaller $e[C(n, t)]$ is, the smaller the sum of squares of the deviations of each class is and the more reasonable the classification.

$e[C(n, t)]$ is calculated using the recursive Equations (15) and (16):

$$e[C(n, 2)] = \min_{2 \leq i \leq n} \{D(1, i - 1) + D(i, n)\} \quad (15)$$

$$e[C(n, t)] = \min_{t \leq i \leq n} \{e[C(i - 1, t - 1)] + D(i, n)\} \quad (16)$$

Step 4: The optimal classification is calculated.

Under the condition that the number of categories t is set, i_t can be found such that the objective function $e[C(n, t)]$ is minimised.

$$e[C(n, t)] = e[C(i_t - 1, t - 1)] + D(i_t, n) \quad (17)$$

The classification $C_t = \{x_{i_t}^*, x_{i_t+1}^*, \dots, x_n^*\}$ is obtained. Further, $i_t - 1$ is found and $e[C(i_t - 1, k - 1)]$ can be calculated using Equation (18):

$$e[C(i_t - 1, k - 1)] = e[C(i_{t-1} - 1, t - 2)] + D(i_{t-1}, i_t - 1) \quad (18)$$

Thus, we obtain $C_{t-1} = \{x_{i_{t-1}}^*, x_{i_{t-1}+1}^*, \dots, x_{i_t-1}^*\}$. All categories C_k , ($k = 1, 2, \dots, t$) can be obtained by analogy.

3. Data Collection

In order to obtain more accurate unit section maintenance requirements for maintenance section classification, this paper proposes a technical condition evaluation index system that includes both pavement surface and pavement internal disease characteristics. The pavement surface technical condition indicators include the pavement condition index (*PCI*), skid resistance index (*SRI*), rut depth index (*RDI*) and ride quality index (*RQI*). The technical indicators for the characterisation of internal pavement distress are the internal pavement crack rate indicators. The length of a unit section in this paper is set to 1000 m [37].

3.1. Project and Materials

This research was based on an expressway named GB1 that was opened to traffic in 2005; it is an important highway section of the Beijing–Hong Kong–Macau Expressway in Guangdong province. The traffic volume has increased rapidly to the current average of 120,000 vehicles per day (converted to passenger cars). Traffic congestion is becoming more and more normal, especially during holidays. Table 1 provides some information on the structure of a typical section. The upper layer of the pavement structure is a 5 cm AK-16 anti-skid wear layer, while the middle layer and lower layer adopt the widely used continuous dense-gradation 6 cm AC-20 and 7 cm AC-25 materials, respectively. The base layer is almost 54 cm of cement-stabilized gravel. In the last five years, some 0.5–2 cm ultra-thin overlays have been successively paved on the upper layer, such as Novachip.

Table 1. Pavement structure information for a typical section.

| Layer | Definition |
|------------------------|------------------------------------------------|
| Asphalt overlay | 0.5–2 cm preventive maintenance measures |
| Upper layer (asphalt) | 5 cm AK-16 (with base binder asphalt) |
| Middle layer (asphalt) | 6 cm AC-20 (with base binder asphalt) |
| Lower layer (asphalt) | 7 cm AC-25 (with base binder asphalt) |
| Base layer | 38 cm stabilized gravel (cement content: 5–6%) |
| Sub-base layer | 16 cm stabilized gravel (cement content: 4%) |
| Subgrade | Soil |

3.2. Data Collection for the Surface Technical Condition

The multifunctional vehicle mainly consisted of a charge-coupled device (CCD) camera system, laser scanner system, GPS system and distance measuring device (DMI). The CCD camera with a resolution of 1920×1080 pixels could simultaneously record images at different angles and identify different kinds of surface diseases. The surveying width was more than 4 m. The vehicle could detect one time period during which the full width of each lane with a width of 3.75 m could be covered in a continuous project. The vehicle speed during detection ranged from 60 km/h to 80 km/h.

The multifunctional vehicle could simultaneously determine the three surface condition indexes (pavement condition index (*PCI*), rut depth index (*RDI*) and riding quality index (*RQI*)), while the skid resistance index (*SRI*) required a special sideways-force coefficient detection vehicle.

3.3. Data Collection for the Pavement Internal Crack Rate

This project used 3D GPR to detect the inner damage affecting pavement structures [38,39]. The 3D GPR used was produced by 3D Radar (Trondheim, Norway) as Figure 1a). The radar host was GEOSCOPE MK IV, and the ground-coupled antennas were the DXG1820 model with a frequency bandwidth of 200–3000 MHz. The utilized 3D GPR could provide 20 emitting and receiving channels for electromagnetic wave signals through a linear combination of 20 pairs of antennas. The separation between antennas was 7.5 cm and the single sampling width for the GPR was 1.5 m. Changes in the GPR's detection parameters caused variations in the vehicle speed during data collection, and the general vehicle speed ranged from 5 km/h to 60 km/h. The trigger spacing was 1 cm, dwell time was $10.0 \mu\text{s}$ and the time window was 25 ns [19]. The software used to process the 3D GPR data was 3D-Radar Examiner 3.5 as Figure 1b).

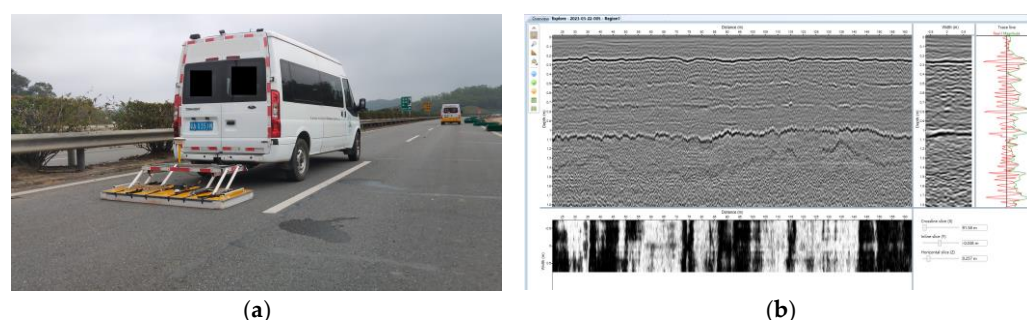


Figure 1. Three-dimensional (3D) GPR detection and analysis: (a) 3D GPR detection; (b) represented result from 3D-Radar Examiner 3.5.

The pavement internal crack rate was utilized to characterize the cracks of the unit sections and calculated using Equation (19) [19]:

$$Cr(i) = 50lc_i/S_i \quad (19)$$

where $Cr(i)$ is the pavement internal crack rate at the depth of h_i (m/100 m²). l_{c_i} is the length of the cracks within a surveying section at the depth of h_i (m). S_i is the surveying area at the depth of h_i (m²).

4. Results and Analysis

In this paper, data for 46 unit sections from the GB1 project were collected using a multifunctional vehicle, sideway-force coefficient detection vehicle and 3D GPR equipment (see Table 2). According to previous studies [40], the life of a semi-rigid-base asphalt pavement is mainly composed of the fatigue cracking life of the semi-rigid base and the fatigue cracking life of the asphalt layer, which is influenced by the integrity (cracking state) of the structural layer. Therefore, this study used the asphalt surface crack rate $Cr(0)$ and the base layer's crack rate as indicators for evaluating the maintenance needs of a unit section. The sum thickness of the whole asphalt layer and the ultra-thin overlay plus 0.05 m was taken as the radar signal pick-up depth for the base layer. Data collected from the GB1 project are listed in Table 2.

Table 2. Pavement condition index.

| Unit Section Number | PCI | SRI | RDI | RQI | Cr(0) | Cr(0.25) |
|---------------------|-----|-----|-----|-----|-------|----------|
| 1 | 74 | 96 | 84 | 94 | 53.0 | 26.0 |
| 2 | 74 | 96 | 84 | 94 | 53.0 | 28.0 |
| 3 | 76 | 99 | 82 | 93 | 0.0 | 39.0 |
| 4 | 86 | 99 | 82 | 97 | 28.7 | 45.0 |
| 5 | 86 | 100 | 85 | 95 | 20.5 | 37.0 |
| 6 | 86 | 100 | 85 | 95 | 20.5 | 18.0 |
| 7 | 86 | 100 | 85 | 95 | 20.5 | 79.0 |
| 8 | 86 | 100 | 85 | 95 | 20.5 | 3.0 |
| 9 | 80 | 100 | 83 | 95 | 18.8 | 28.0 |
| 10 | 80 | 100 | 83 | 95 | 18.8 | 65.0 |
| 11 | 80 | 100 | 83 | 95 | 18.8 | 0.0 |
| 12 | 86 | 98 | 83 | 95 | 9.0 | 14.0 |
| 13 | 82 | 99 | 84 | 94 | 15.1 | 12.0 |
| 14 | 82 | 99 | 84 | 94 | 15.1 | 56.0 |
| 15 | 80 | 99 | 85 | 94 | 15.5 | 74.0 |
| 16 | 80 | 99 | 85 | 94 | 15.5 | 65.0 |
| 17 | 85 | 99 | 84 | 95 | 11.7 | 57.0 |
| 18 | 85 | 99 | 84 | 95 | 11.7 | 44.0 |
| 19 | 88 | 97 | 83 | 95 | 17.7 | 50.0 |
| 20 | 97 | 99 | 82 | 93 | 14.5 | 57.0 |
| 21 | 97 | 99 | 82 | 93 | 14.5 | 45.0 |
| 22 | 93 | 98 | 84 | 95 | 7.1 | 38.0 |
| 23 | 93 | 98 | 84 | 95 | 7.1 | 11.0 |
| 24 | 93 | 98 | 84 | 95 | 7.1 | 31.0 |
| 25 | 87 | 93 | 81 | 95 | 15.5 | 42.0 |
| 26 | 87 | 93 | 81 | 95 | 15.5 | 21.0 |
| 27 | 85 | 98 | 84 | 96 | 14.4 | 6.0 |
| 28 | 84 | 98 | 83 | 95 | 14.0 | 50.0 |
| 29 | 90 | 98 | 85 | 93 | 8.1 | 9.0 |
| 30 | 90 | 98 | 85 | 93 | 8.1 | 39.0 |
| 31 | 84 | 98 | 82 | 93 | 12.2 | 73.0 |

Table 2. Cont.

| Unit Section Number | PCI | SRI | RDI | RQI | Cr(0) | Cr(0.25) |
|---------------------|-----|-----|-----|-----|-------|----------|
| 32 | 100 | 93 | 82 | 97 | 4.5 | 44.0 |
| 33 | 94 | 98 | 85 | 95 | 12.4 | 2.0 |
| 34 | 100 | 97 | 84 | 94 | 4.1 | 59.0 |
| 35 | 100 | 97 | 84 | 94 | 4.1 | 79.0 |
| 36 | 93 | 99 | 83 | 95 | 12.9 | 20.0 |
| 37 | 81 | 98 | 85 | 94 | 14.8 | 37.0 |
| 38 | 81 | 98 | 85 | 94 | 14.8 | 25.0 |
| 39 | 81 | 98 | 85 | 94 | 14.8 | 32.0 |
| 40 | 88 | 98 | 84 | 94 | 13.9 | 5.0 |
| 41 | 93 | 98 | 84 | 94 | 10.0 | 41.0 |
| 42 | 93 | 98 | 84 | 94 | 10.0 | 74.0 |
| 43 | 93 | 98 | 84 | 94 | 10.0 | 77.0 |
| 44 | 93 | 98 | 84 | 94 | 10.0 | 39.0 |
| 45 | 100 | 100 | 82 | 95 | 0.2 | 43.0 |
| 46 | 96 | 96 | 85 | 98 | 0.0 | 47.0 |

4.1. Principal Components Analysis

There is often a certain correlation between the pavement performance indicators during service life; for example, ride quality indicators are often influenced by rutting indicators. This eliminates the requirement to subject all the metrics collected to calculation to assess the need for pavement maintenance, saving computing resources. The principal component analysis (PCA) technique is a commonly used method of data dimensionality reduction [41,42].

(1) Applicability test for PCA

Principal component factor analysis was performed for the six technical indicators (shown in Table 2) in this study using the Kaiser–Meyer–Olkin test and Barlett’s test of sphericity [43]. The test model is shown by Equation (20):

$$KMO = \begin{cases} \geq 0.5, OK \\ < 0.5, Not OK \end{cases} \left(KMO = \frac{\sum \sum_{i \neq j} r_{ij}^2}{\sum \sum_{i \neq j} r_{ij}^2 + \sum \sum_{i \neq j} \alpha_{ij}^2} \right) \quad (20)$$

where r_{ij} , and α_{ij} are, respectively, the simple and bias correlation coefficients for each pair of indicators in Table 2. The correlation matrix for the PCA is shown in Table 3.

As can be seen from Table 3, the absolute values of the cross-correlation coefficients for the six technical indicators ranged from 0.033 to 0.617, with the correlation coefficient between PCI and $Cr(0)$ being the largest and most significant; thus, it can be presumed that the main surface disease affecting the GB1 project is cracking. Secondly, the correlation between RDI and RQI was also somewhat significant, in line with the engineering understanding that rutting has some effect on the ride quality provided by a road surface. The result of the KMO test was $0.517 > 0.5$ and the result of Barlett’s test of sphericity was $p < 0.05$ (p value of 0.003), thus, the six technical indicators were judged to be suitable for principal component analysis.

Table 3. Correlation matrix for PCA.

| Correlation Coefficient | PCI | SRI | RDI | RQI | Cr(0) | Cr(0.25) |
|-------------------------|--------------------|--------|--------------------|--------------------|--------------------|----------|
| PCI | 1.000 | 0.162 | −0.136 | −0.181 | −0.617 | 0.158 |
| SRI | 0.162 | 1.000 | −0.074 | −0.206 | −0.044 | −0.143 |
| RDI | −0.136 | −0.074 | 1.000 | 0.341 | 0.064 | −0.082 |
| RQI | −0.181 | −0.206 | 0.341 | 1.000 | −0.033 | 0.011 |
| Cr(0) | −0.617 | −0.044 | 0.064 | −0.033 | 1.000 | −0.153 |
| Cr(0.25) | 0.158 | −0.143 | −0.082 | 0.011 | −0.153 | 1.000 |
| Significance | PCI | SRI | RDI | RQI | Cr(0) | Cr(0.25) |
| PCI | | 0.141 | 0.184 | 0.115 | 0.000 ^a | 0.146 |
| SRI | 0.141 | | 0.312 | 0.084 | 0.386 | 0.171 |
| RDI | 0.184 | 0.312 | | 0.010 ^b | 0.337 | 0.293 |
| RQI | 0.115 | 0.084 | 0.010 ^b | | 0.414 | 0.472 |
| Cr(0) | 0.000 ^a | 0.386 | 0.337 | 0.414 | | 0.154 |
| Cr(0.25) | 0.146 | 0.171 | 0.293 | 0.472 | 0.154 | |

Note: ^a significance p -value < 0.01, ^b significance p -value < 0.05.

(2) Principal component retention

The GB1 measured sample data matrix $X = \{X_j\}, (j = 1, 2, \dots, 6)$ was normalized according to Equation (2) to obtain $X^* = \{X_j^*\}, (j = 1, 2, \dots, 6)$. Then, we calculated the data correlation matrix $R(X^*) = R(X)$ (see Table 3). The eigenvalues of $R(X^*)$ were calculated from $|R(X^*) - \lambda E| = 0$ and are shown in Table 4. Each eigenvalue corresponded to a principal component $Z_\zeta, (\zeta = 1, 2, \dots, 6)$, and the cumulative contribution of Z_ζ was calculated from $c_\zeta = \sum_{j=1}^{\zeta} \lambda_j / \sum_{j=1}^6 \lambda_j$ (see Table 4). The eigenvectors corresponding to the eigenvalues of $R(X^*)$ were also calculated from $|R(X^*) - \lambda E| = 0$, and the eigenvectors are listed in Table 5.

Table 4. Eigenvalues of correlation matrix.

| Principal Component | Eigenvalues, λ_j | Cumulative Contribution Rate, $c_\zeta/\%$ |
|---------------------|--------------------------|--------------------------------------------|
| Z_1 | 1.808 | 30.128 |
| Z_2 | 1.362 | 52.826 |
| Z_3 | 1.089 | 70.974 |
| Z_4 | 0.761 | 83.662 |
| Z_5 | 0.637 | 94.278 |
| Z_6 | 0.343 | 100.000 |

Table 5. Eigenvectors corresponding to the eigenvalues.

| Index | Z_1 | Z_2 | Z_3 | Z_4 | Z_5 | Z_6 |
|---------|--------|--------|--------|--------|--------|--------|
| E_1^* | 0.632 | 0.190 | −0.180 | 0.089 | 0.171 | 0.704 |
| E_2^* | 0.227 | −0.419 | −0.539 | −0.605 | −0.334 | −0.071 |
| E_3^* | −0.324 | 0.417 | −0.474 | −0.326 | 0.622 | −0.053 |
| E_4^* | −0.311 | 0.584 | −0.204 | 0.011 | −0.683 | 0.233 |
| E_5^* | −0.549 | −0.397 | 0.204 | −0.231 | 0.072 | 0.664 |
| E_6^* | 0.216 | 0.340 | 0.608 | −0.683 | −0.014 | −0.041 |

From Tables 4 and 5, it can be seen that, when the four principal components Z_1, Z_2, Z_3 and Z_4 were selected, their variance accounted for about 84% of the total variance, indicating that these four principal components were able to retain about 84% of the information from the original data matrix. The principal component matrix was obtained using Equation (21), and the model of the relationship with the original variables is shown in Equation (22):

$$Z = \{Z_{i\zeta}\} \quad (21)$$

$$Z_{i\zeta} = \sum_{j=1}^{\zeta} E_j^* X_{ij}, (i = 1, 2, \dots, n; \zeta = 1, 2, 3, 4) \quad (22)$$

(3) Principal component matrix

For the GB1 project, the principal component scores for each unit section were calculated according to Equations (21) and (22), as shown in Table 6.

Table 6. Scores for principal components.

| Unit Section Number | Z ₁ | Z ₂ | Z ₃ | Z ₄ |
|---------------------|----------------|----------------|----------------|----------------|
| 1 | -11.371 | 51.559 | -97.436 | -107.845 |
| 2 | -10.939 | 52.239 | -96.220 | -109.211 |
| 3 | 23.438 | 74.725 | -101.169 | -105.477 |
| 4 | 14.081 | 69.627 | -94.292 | -115.259 |
| 5 | 16.715 | 69.814 | -102.376 | -109.513 |
| 6 | 12.611 | 63.354 | -113.928 | -96.536 |
| 7 | 25.787 | 84.094 | -76.840 | -138.199 |
| 8 | 9.371 | 58.254 | -123.048 | -86.291 |
| 9 | 12.577 | 65.467 | -106.173 | -102.848 |
| 10 | 20.569 | 78.047 | -83.677 | -128.119 |
| 11 | 6.529 | 55.947 | -123.197 | -83.724 |
| 12 | 18.260 | 66.568 | -116.682 | -89.283 |
| 13 | 12.171 | 62.124 | -116.745 | -90.622 |
| 14 | 21.675 | 77.084 | -89.993 | -120.674 |
| 15 | 23.761 | 83.086 | -79.083 | -133.562 |
| 16 | 21.817 | 80.026 | -84.555 | -127.415 |
| 17 | 25.337 | 79.924 | -90.820 | -120.296 |
| 18 | 22.529 | 75.504 | -98.724 | -111.417 |
| 19 | 22.303 | 76.157 | -92.842 | -115.095 |
| 20 | 32.638 | 79.079 | -91.047 | -119.252 |
| 21 | 30.046 | 74.999 | -98.343 | -111.056 |
| 22 | 28.588 | 77.229 | -104.212 | -104.939 |
| 23 | 22.756 | 68.049 | -120.628 | -86.498 |
| 24 | 27.076 | 74.849 | -108.468 | -100.158 |
| 25 | 20.869 | 74.947 | -94.863 | -106.150 |
| 26 | 16.333 | 67.807 | -107.631 | -91.807 |
| 27 | 12.312 | 62.523 | -120.947 | -85.466 |
| 28 | 21.995 | 76.419 | -93.402 | -115.218 |
| 29 | 20.144 | 65.627 | -121.153 | -85.992 |
| 30 | 26.624 | 75.827 | -102.913 | -106.482 |
| 31 | 28.897 | 83.369 | -78.903 | -130.207 |
| 32 | 34.637 | 84.068 | -99.123 | -104.110 |
| 33 | 18.182 | 63.472 | -125.662 | -81.824 |
| 34 | 39.279 | 86.725 | -92.573 | -117.372 |
| 35 | 43.599 | 93.525 | -80.413 | -131.032 |
| 36 | 22.039 | 67.951 | -114.027 | -94.276 |
| 37 | 16.514 | 71.361 | -101.347 | -107.454 |
| 38 | 13.922 | 67.281 | -108.643 | -99.258 |
| 39 | 15.434 | 69.661 | -104.387 | -104.039 |
| 40 | 14.861 | 61.764 | -121.778 | -84.434 |
| 41 | 27.922 | 76.490 | -101.580 | -107.683 |
| 42 | 35.050 | 87.710 | -81.516 | -130.222 |
| 43 | 35.698 | 88.730 | -79.692 | -132.271 |
| 44 | 27.490 | 75.810 | -102.796 | -106.317 |
| 45 | 38.976 | 81.323 | -103.967 | -106.698 |
| 46 | 34.598 | 86.673 | -100.730 | -108.269 |

As can be seen from Table 6, the original six variables *PCI*, *SRI*, *RDI*, *RQI*, *Cr(0)* and *Cr(0.25)* were turned into the four principal component variables *Z₁*, *Z₂*, *Z₃* and *Z₄* using principal component analysis, achieving a reduction of over 33% in the number of variables while retaining over 84% of the information in the original variables.

4.2. Analysis of Clustering Results

The systematic clustering, dynamic clustering and ordered clustering analysis methods mentioned in Section 2 were used to cluster the original variable data matrix $\{X_1, \dots, X_6\}$,

surface technical condition data $\{X_1, \dots, X_4\}$ and principal components $\{Z_1, \dots, Z_4\}$, respectively, in order to investigate the influence of the clustering methods, principal component analysis and pavement internal crack rate on the results of the section classification.

Considering that the asphalt pavement maintenance planning cycle generally lasts five years, the number of clusters in this was uniformly set to five. The results for the 46 unit sections classified for the GB1 project are shown in Table 7.

Table 7. Clustering results for 46 unit sections for the GB1 project.

| Clustering Method | Category 1 | Category 2 | Category 3 | Category 4 | Category 5 | |
|-----------------------|-------------|----------------------------------------|-----------------------------------|------------------------------------------|------------------------------------------|----------------------------------------|
| Systematic clustering | $X_1 - X_4$ | 1–3 | 4–19, 22–24, 27–31, 33, 36–44, 46 | 20–21, 34–35, 45 | 25–26 | 32 |
| | $X_1 - X_6$ | 1–2 | 3 | 4 | 5–19, 21–33, 35–46 | 20, 34 |
| | $Z_1 - Z_4$ | 1–2 | 3, 5–31, 33, 35–44 | 4 | 32, 45–46 | 34 |
| Dynamic clustering | $X_1 - X_4$ | 1–3, 9–11, 13–16, 37–39 | 32, 46 | 4–8, 12, 17–19, 25–28, 31, 40 | 20–21, 34–35, 45 | 22, 24, 29–30, 33, 36, 41–44 |
| | $X_1 - X_6$ | 6, 8, 11–13, 23, 26–27, 29, 33, 36, 40 | 1–2 | 3–5, 9, 18, 22, 24–25, 30, 37–39, 41, 44 | 7, 10, 15–16, 31, 35, 42–43 | 14, 17, 19–21, 28, 32, 34, 45–46 |
| | $Z_1 - Z_4$ | 14, 17, 19–21, 28, 32, 34, 45–46 | 1–2 | 7, 10, 15–16, 31, 35, 42–43 | 3–5, 9, 18, 22, 24–25, 30, 37–39, 41, 44 | 6, 8, 11–13, 23, 26–27, 29, 33, 36, 40 |
| Ordered clustering | $X_1 - X_4$ | 1–33 | 34 | 35–38 | 39–45 | 46 |
| | $X_1 - X_6$ | 1–9 | 10–13 | 14–25 | 26–28 | 29–46 |
| | $Z_1 - Z_4$ | 1–12 | 13 | 14–25 | 26–44 | 45–46 |

As shown in Table 7, there were significant differences in the classification results of the various clustering methods. The results using the principal components $\{Z_1, \dots, Z_4\}$ and $\{X_1, \dots, X_6\}$ had a relatively high degree of overlap, which side-by-side verified the ability of the PCA to retain information about the original data.

Box plots indicating the statistical distribution of each technical indicator for different combinations of clustered data and different clustering methods and principal component techniques are shown in Figures 2–10. These figures show the mean value and the range of distribution for each technical indicator in each of the five categories. Using Figure 2 as an example, the means of $Cr(0)$ and $Cr(0.25)$ were relatively distinctly different, while the means of PCI , SRI , RDI and RQI were very similar. The graphs could reflect the variability of the results under the scheme using the data matrix $\{X_1, \dots, X_6\}$ with the application of the hierarchical clustering method.

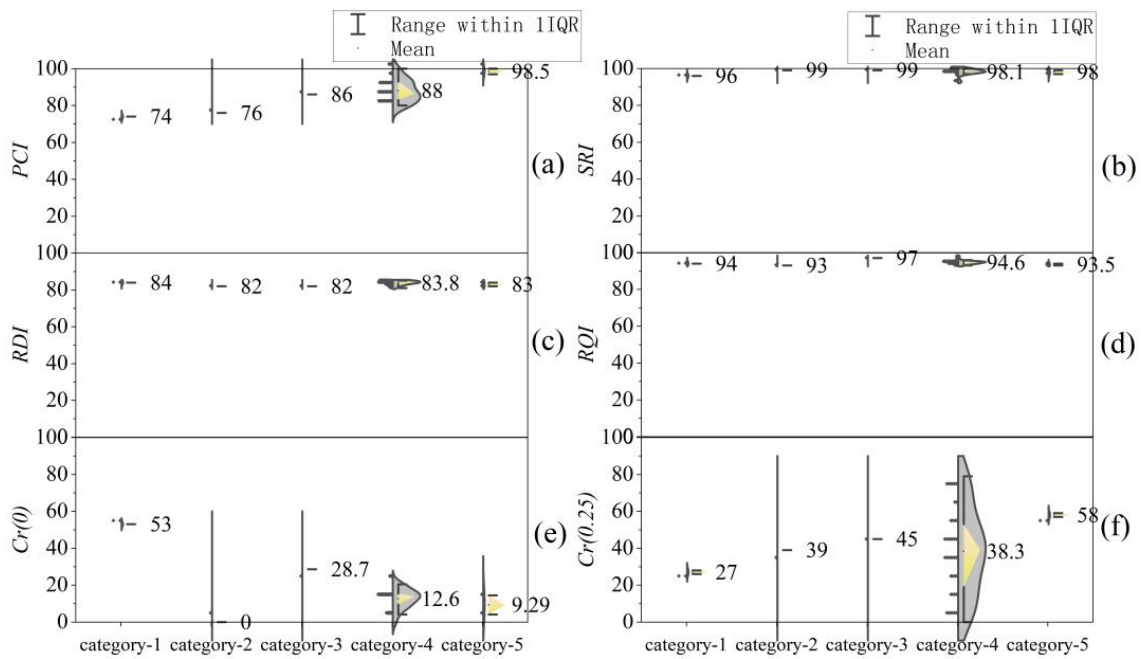


Figure 2. Distribution of the different technical indicators of the classification results using data matrix $\{X_1, \dots, X_6\}$ with the application of the hierarchical clustering method: (a) *PCI*; (b) *SRI*; (c) *RDI*; (d) *RQI*; (e) $Cr(0)$; (f) $Cr(0.25)$.

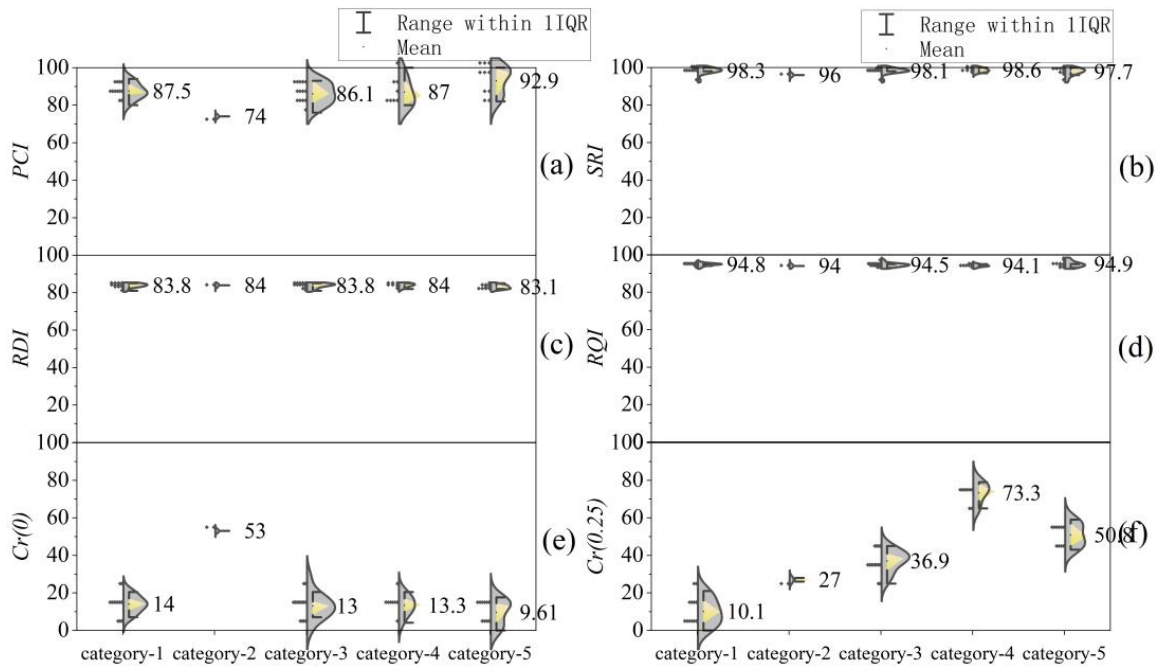


Figure 3. Distribution of the different technical indicators of the classification results using data matrix $\{X_1, \dots, X_6\}$ with the application of the dynamic clustering method: (a) *PCI*; (b) *SRI*; (c) *RDI*; (d) *RQI*; (e) $Cr(0)$; (f) $Cr(0.25)$.

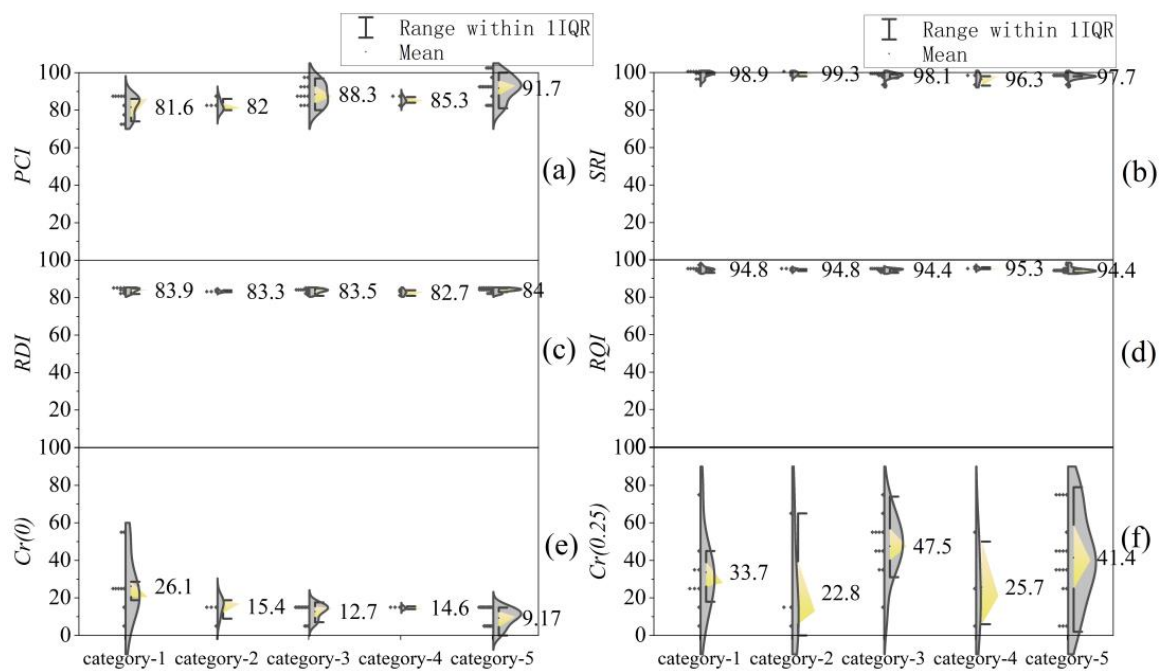


Figure 4. Distribution of the different technical indicators of the classification results using data matrix $\{X_1, \dots, X_6\}$ with the application of the ordered clustering method: (a) PCI; (b) SRI; (c) RDI; (d) RQI; (e) Cr(0); (f) Cr(0.25).

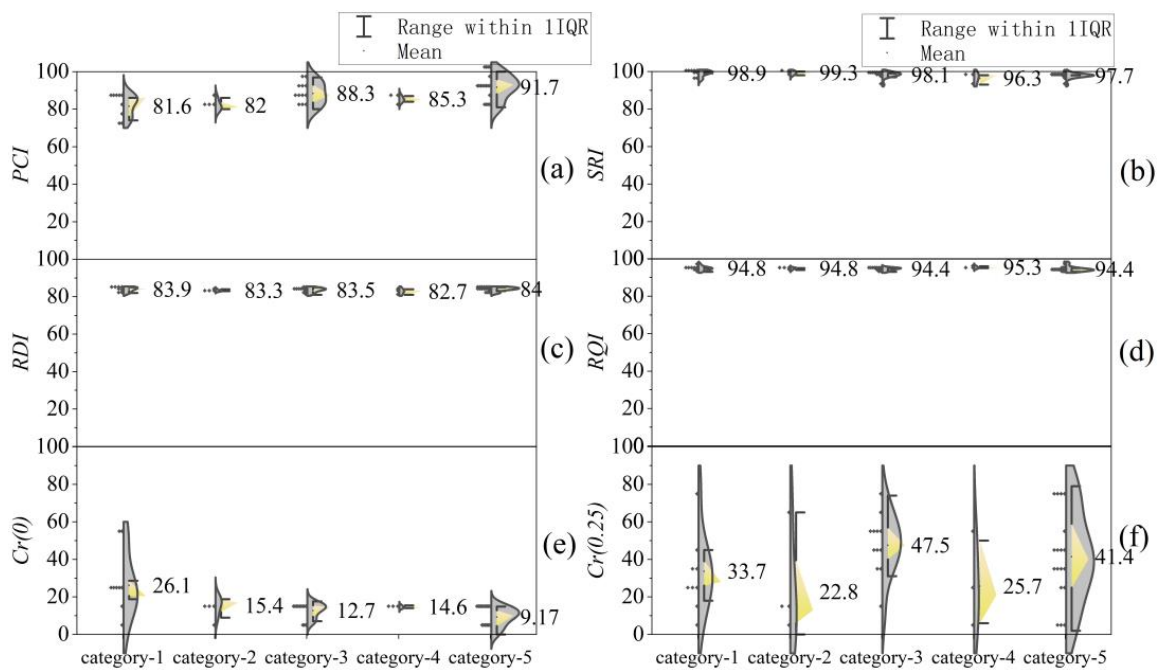


Figure 5. Distribution of the different technical indicators of the classification results using data matrix $\{X_1, \dots, X_4\}$ with the application of the hierarchical clustering method: (a) PCI; (b) SRI; (c) RDI; (d) RQI; (e) Cr(0); (f) Cr(0.25).

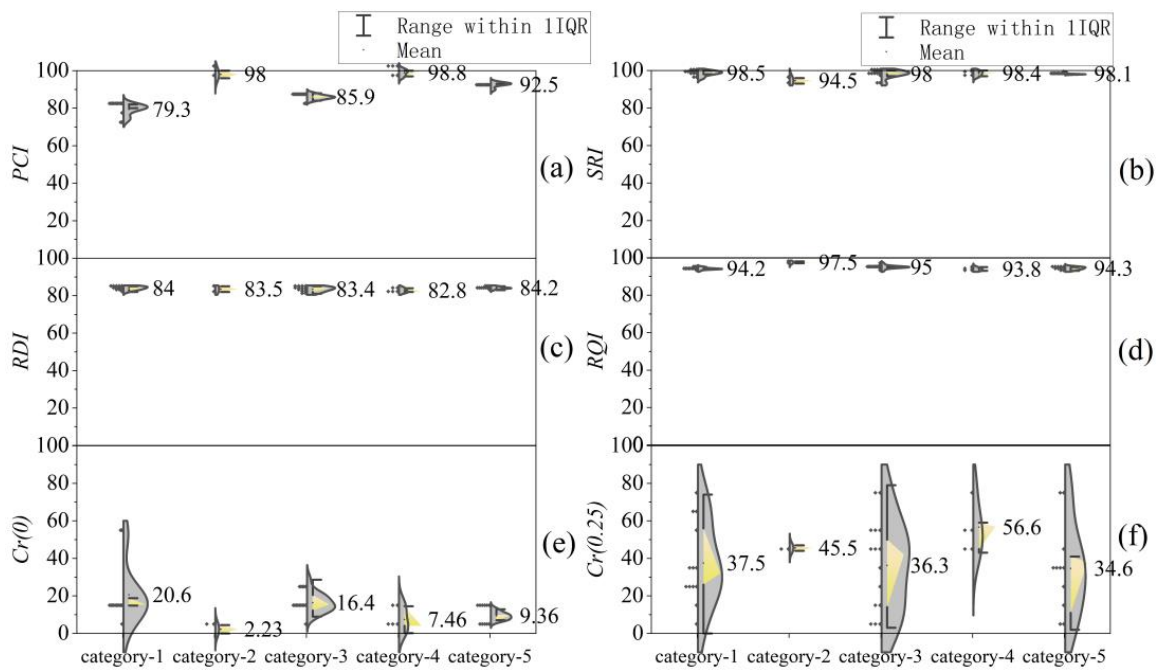


Figure 6. Distribution of the different technical indicators of the classification results using data matrix $\{X_1, \dots, X_4\}$ with the application of the dynamic clustering method: (a) *PCI*; (b) *SRI*; (c) *RDI*; (d) *RQI*; (e) $Cr(0)$; (f) $Cr(0.25)$.

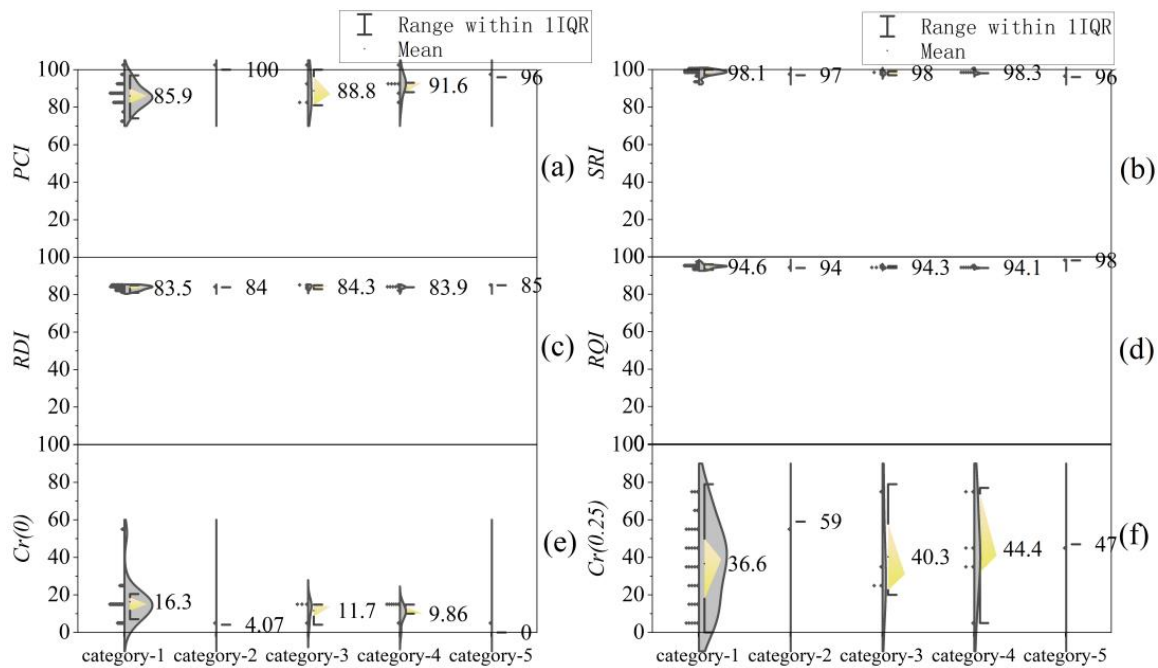


Figure 7. Distribution of the different technical indicators of the classification results using data matrix $\{X_1, \dots, X_4\}$ with the application of the ordered clustering method: (a) *PCI*; (b) *SRI*; (c) *RDI*; (d) *RQI*; (e) $Cr(0)$; (f) $Cr(0.25)$.

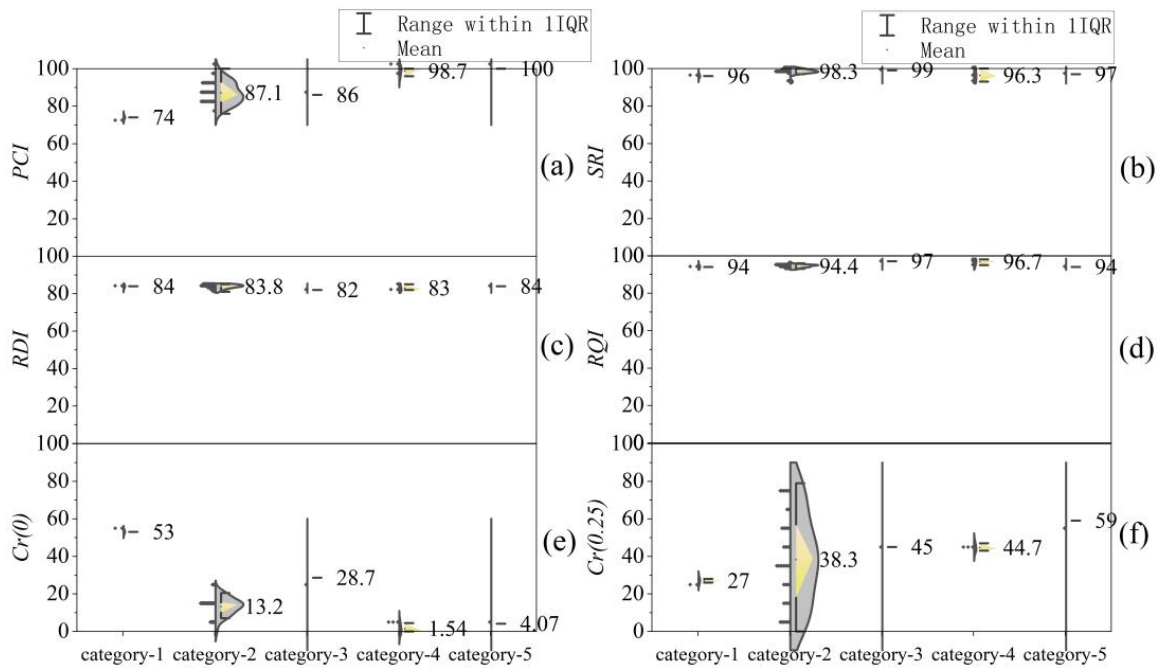


Figure 8. Distribution of the different technical indicators of the classification results using data matrix $\{Z_1, \dots, Z_4\}$ with the application of the hierarchical clustering method and PCA: (a) PCI; (b) SRI; (c) RDI; (d) RQI; (e) $Cr(0)$; (f) $Cr(0.25)$.

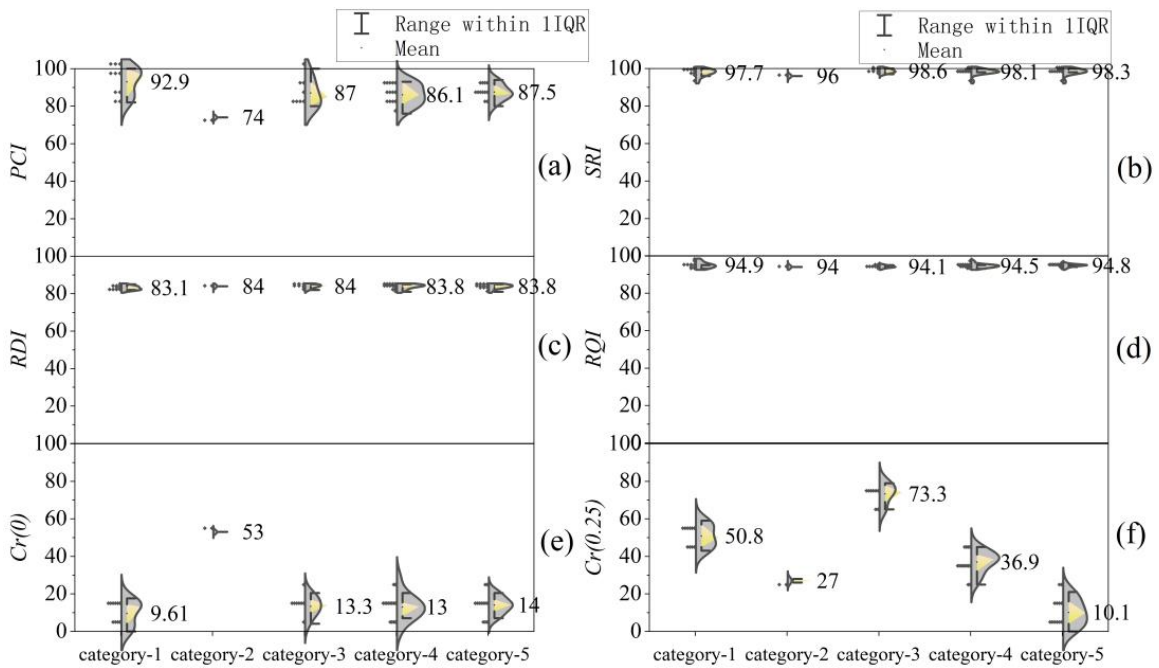


Figure 9. Distribution of the different technical indicators of the classification results using data matrix $\{Z_1, \dots, Z_4\}$ with the application of the dynamic clustering method and PCA: (a) PCI; (b) SRI; (c) RDI; (d) RQI; (e) $Cr(0)$; (f) $Cr(0.25)$.

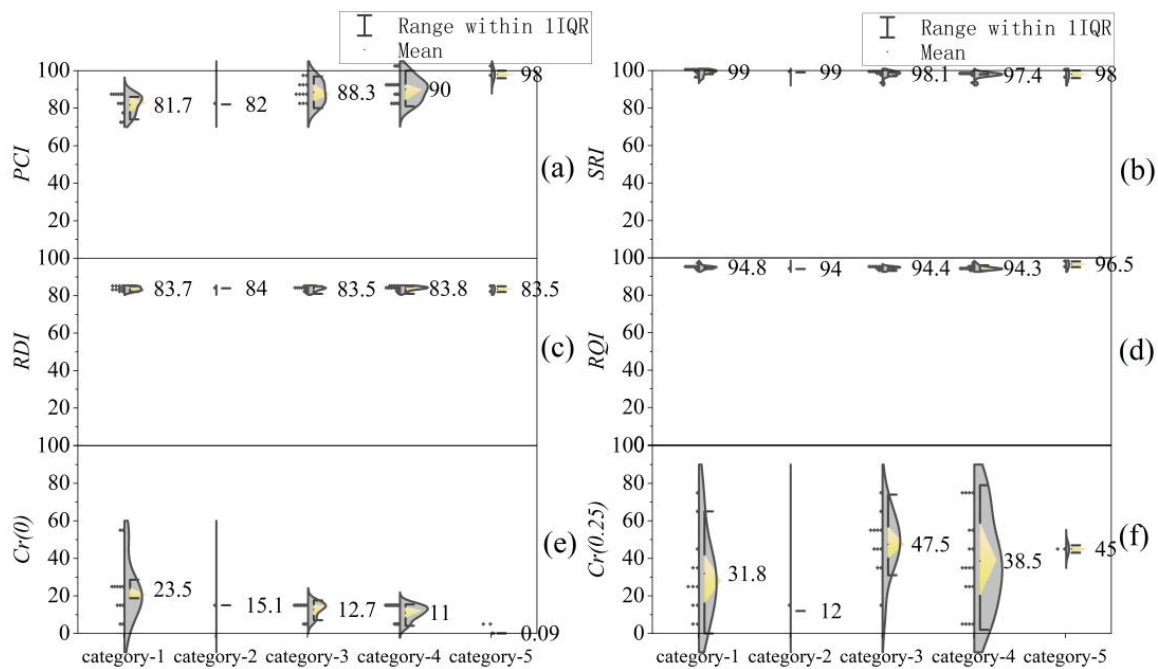


Figure 10. Distribution of the different technical indicators of the classification results using data matrix $\{Z_1, \dots, Z_4\}$ with the application of the ordered clustering method and PCA: (a) *PCI*; (b) *SRI*; (c) *RDI*; (d) *RQI*; (e) *Cr(0)*; (f) *Cr(0.25)*.

As shown by Figures 2–10, the results obtained by the different clustering methods did not necessarily differ when analysing their individual specific indicators. In addition, when the ordered clustering method was utilized, the mean values and distribution ranges of the technical indicators obtained for each clustered sub-section were less differentiated, regardless of the type of clustered data used and regardless of whether the principal component method was used. When the hierarchical clustering method was used, the differentiation of indicator *PCI* in the clustered sub-sections was better. When the dynamic clustering method was used, the differentiation of *Cr(0.25)* in the clustered sub-sections was better. In terms of the selection of clustered data, when the clustered data did not contain *Cr(0)* and *Cr(0.25)*, *Cr(0)* and *Cr(0.25)* also did not appear in the clustered results for indicators with high differentiation.

The ultimate goal of clustering is to classify the most similar unit sections into a particular sub-section. In order to more objectively compare the advantages and disadvantages of different clustering methods, a statistical ANOVA was conducted for the data for each technical index of the sub-sections classified by different clustering methods, and a *p*-value was used to characterise the significance of the differences between the data of each sub-section (see Figure 11). Statistically, the smaller the *p*-value, the more significant the differences between the data for each sub-section will be.

As can be seen from Figure 11, there was a genetic relationship between the clustering base data characteristics and the technical characteristics of the delineated sub-sections. When using $\{X_1, \dots, X_6\}$ and $\{Z_1, \dots, Z_4\}$, the *p*-values for *Cr(0.25)* obtained by the dynamic and ordered clustering methods were significantly larger than those obtained by using $\{X_1, \dots, X_4\}$. The sub-sections resulting from $\{X_1, \dots, X_4\}$ did not reflect the differential characteristics of *Cr(0.25)*, which was related to the fact that the underlying data used for the clustering segments did not contain *Cr(0.25)*. *Cr(0)* also exhibited similar characteristics, with the *p*-values from $\{X_1, \dots, X_6\}$ and $\{Z_1, \dots, Z_4\}$ being significantly smaller than that from $\{X_1, \dots, X_4\}$, and this pattern held true for the systematic clustering approach as well. This result suggests that, when classifying asphalt pavements, if the difference in the technical characteristics of an aspect of the asphalt pavement is to be reflected in the classified section, it is necessary to include that technical indicator in the

construction of the clustering data matrix, such as with $Cr(0)$ and $Cr(0.25)$ studied in this paper.

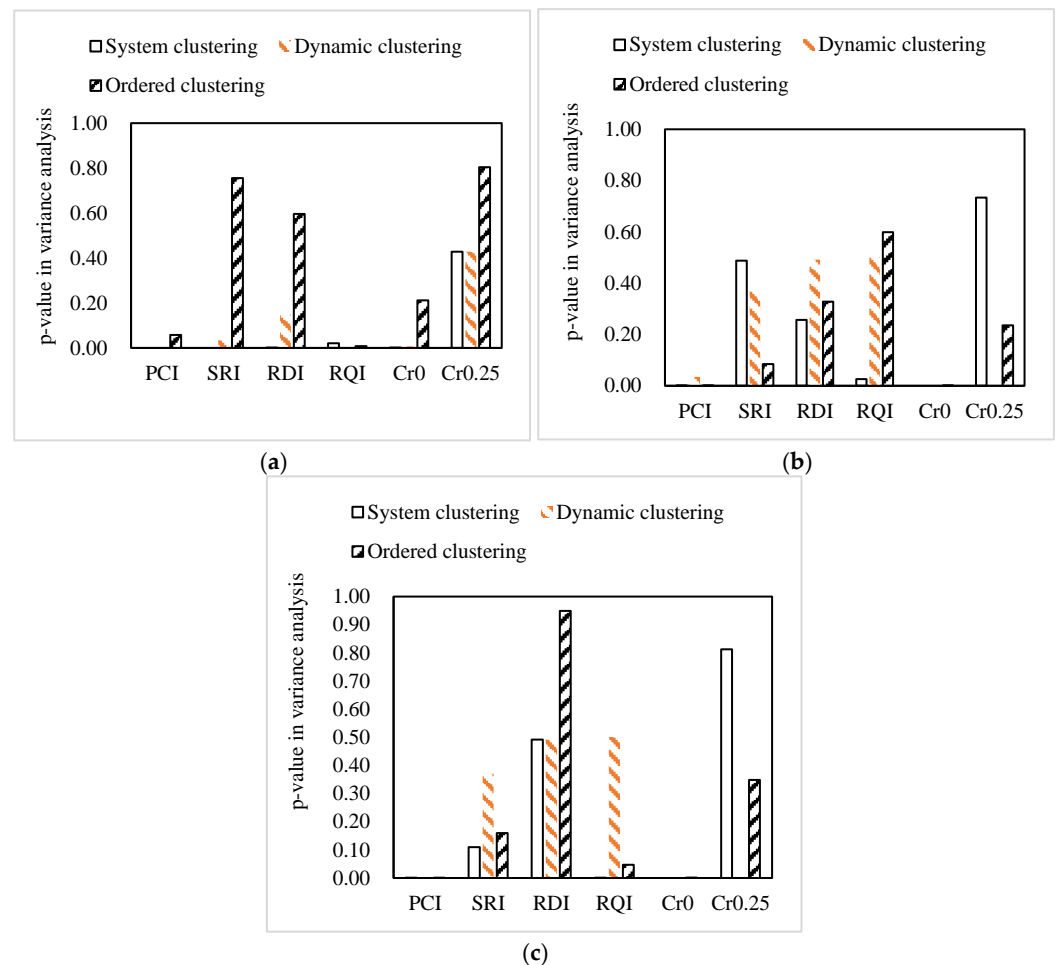


Figure 11. Significance of the differences in the results obtained with different clustering data by different clustering methods: (a) using data for X_1-X_4 ; (b) using data for X_1-X_6 ; (c) using data for Z_1-Z_4 .

According to the results in Table 3, PCI and $Cr(0)$ were the most significantly correlated, so they reflected essentially the same pattern of data. However, the p -values of the clustering results for indicators SRI , RDI and RQI did not reflect a similar pattern as for PCI , $Cr(0)$ and $Cr(0.25)$. In particular, for SRI , the p -values of $\{X_1, \dots, X_6\}$ and $\{Z_1, \dots, Z_4\}$ were significantly greater for the systematic and dynamic clustering methods than that of $\{X_1, \dots, X_4\}$, but the results were reversed when the ordered clustering method was used. For RDI , the ordered clustering method resulted in significantly larger p -values for $\{Z_1, \dots, Z_4\}$ than for $\{X_1, \dots, X_6\}$ and $\{X_1, \dots, X_4\}$, while the systematic and dynamic clustering methods resulted in significantly larger p -values for $\{X_1, \dots, X_6\}$ and $\{Z_1, \dots, Z_4\}$ than that for $\{X_1, \dots, X_4\}$. For RQI , dynamic and ordered clustering methods showed significantly larger p -values for $\{X_1, \dots, X_6\}$ and $\{Z_1, \dots, Z_4\}$ than for the segmentation results for $\{X_1, \dots, X_4\}$.

In general, there were certain applicable relationships between the different clustering methods and the clustered data.

4.3. Applicability of Clustering Methods

In the practice of asphalt pavement maintenance and management, managers usually wish to design maintenance plans according to consecutive ordered segments, as this

makes it more convenient and easier to allocate maintenance resources (which involve the transportation of construction materials, equipment and personnel, traffic organisation and other management issues), and consecutive segments are more conducive to mechanised operations and maintenance and repair quality assurance. Therefore, the ordered clustering method has been the more widely recommended method. However, as shown by Figure 11, although the ordered clustering method maximised the continuous and ordered merging of the different unit sections, the final clustering results did not guarantee that the technical characteristics of each sub-section were in a significantly different state after clustering. Five of the seven indicators (more than 71%) from the ordered clustering results in Figure 11a had higher p -value levels than in the systematic and dynamic clustering. The technical disadvantage of the ordered clustering method is that it tends to make it difficult to differentiate the maintenance plans for each sub-section, and it is not suitable for projects that require a high degree of refinement in the technical requirements of the maintenance plans. However, for projects that are limited by traffic volumes or other management factors, the ordered clustering method can be used.

Observing Figure 11, it can be seen that the p -value levels with the systematic clustering method were lower than 0.05 for all indicators except the indicator when clustering the segmentation of $\{X_1, \dots, X_4\}$ (see Figure 11a). In addition, when applying the systematic clustering method, adding the internal crack rate to the data matrix caused significantly higher p -values for indicators SRI , RDI and $Cr(0.25)$ for different sub-sections (see Figure 11a,b). Combining the functional indicators and the internal crack rate when classifying pavement sections using the systematic clustering method may have negative effects. Therefore, for projects that focus only on the surface functional indicators, a systematic clustering approach is advantageous.

The dynamic clustering method is suitable for projects that focus on the impact of the internal pavement condition on pavement maintenance needs. Adding the internal crack rate indicator resulted in significantly higher p -values for indicators PCI , SRI , RDI and RQI for different sub-sections but also significantly reduced the p -values for indicators $Cr(0)$ and $Cr(0.25)$, allowing the clustering to delineate sub-sections that could better reflect the differentiation of the internal disease characteristics of the asphalt pavements (see Figure 11a,b). The dynamic clustering method combined with principal component analysis could significantly improve the significance of the differences for the indicators of interest ($Cr(0)$ and $Cr(0.25)$) in the clustering results. It could also further reduce the p -values of the indicators not of interest (PCI , SRI , RDI and RQI) in the clustering results (see Figure 11b,c), effectively improving the segmentation of asphalt pavement maintenance sections.

5. Conclusions

To classify pavement maintenance sections, a clustering method based on 3D GPR and principal component analysis was proposed in this work. The effects of the clustering methods, principal component analysis and pavement internal crack rate on the classification results were investigated by analysing the significance of the variations in the classification results. The conclusions are as follows.

- (1) The characteristics of the cluster data and the technical characteristics of the subdivisions are genetically related. A clustering data matrix that takes into account internal cracking rates is essential in order to provide an effective means of classifying differences in asphalt pavement performance or maintenance requirements;
- (2) Classification results vary considerably between clustering methods and the choice of clustering method is related to pavement maintenance objectives. Ordered clustering is not suitable for projects requiring sophisticated maintenance plans, whereas it could be considered for traffic-limited projects. For projects focusing on surface functional indicators only, systematic clustering is advantageous, but combining functional and internal crack rates may be counterproductive. Dynamic clustering is suitable for projects focusing on internal distress effects;

- (3) Principal component analysis could reduce data matrix dimensionality by 33% and retain more than 84% of the information. The dynamic clustering method combined with the principal component analysis could significantly improve the significance of the differences for the indicators of interest in the clustering results, as well as the indicators not of interest, effectively improving the classification of asphalt pavement maintenance sections.

The limitations of this study were that limited data from one project were used for the analysis, but the data need to be more representative, and a more in-depth analysis will be conducted using data from multiple projects in the future. The application and validation of the asphalt pavement maintenance section classification method studied in this paper in maintenance science decision making will be followed up.

Author Contributions: Conceptualization, C.X. and J.Y.; methodology, C.X.; investigation, H.L., J.Z., W.L. and J.D.; formal analysis, C.X., H.L., J.Z. and W.L.; writing—original draft, J.D.; writing—review and editing, H.L. and C.X. All authors have read and agreed to the published version of the manuscript.

Funding: The authors would like to acknowledge the financial support provided by the National Natural Science Foundation of China (52178426), the Fundamental Research Funds for the Central Universities (2022ZYGXZR066 and 2023ZYGXZR001) and the Special Project of Foshan Science and Technology Innovation Team (2120001010776).

Data Availability Statement: The data presented in this study are available on request from the corresponding author.

Acknowledgments: The authors would also like to acknowledge the project data support from Guangdong Highway Construction Co., Ltd.

Conflicts of Interest: The authors declare no conflict of interest.

References

- Peterson, J.C.; Bourgin, D.D.; Agrawal, M.; Reichman, D.; Griffiths, T.L. Using large-scale experiments and machine learning to discover theories of human decision-making. *Science* **2021**, *372*, 1209–1214. [[CrossRef](#)] [[PubMed](#)]
- Davids, E.L. The Interaction between Basic Psychological Needs, Decision-Making and Life Goals among Emerging Adults in South Africa. *Soc. Sci.* **2022**, *11*, 316. [[CrossRef](#)]
- Babashamsi, P.; Khahro, S.H.; Omar, H.A.; Al-Sabaei, A.M.; Memon, A.M.; Milad, A.; Khan, M.I.; Sutanto, M.H.; Yusoff, N.I. Perspective of Life-Cycle Cost Analysis and Risk Assessment for Airport Pavement in Delaying Preventive Maintenance. *Sustainability* **2022**, *14*, 2905. [[CrossRef](#)]
- Mousa, M.R.; Elseifi, M.A.; Zhang, Z.; Gaspard, K. Development of a Decision-Making Tool to Select Optimum Preventive Maintenance Treatments in a Hot and Humid Climate. *Transp. Res. Rec. J. Transp. Res. Board* **2020**, *2674*, 44–56. [[CrossRef](#)]
- Miah, M.T.; Oh, E.; Chai, G.; Bell, P. An overview of the airport pavement management systems (APMS). *Int. J. Pavement Res. Technol.* **2021**, *13*, 581–590. [[CrossRef](#)]
- Fani, A.; Golroo, A.; Mirhassani, S.A.; Gandomi, A.H. Pavement maintenance and rehabilitation planning optimisation under budget and pavement deterioration uncertainty. *Int. J. Pavement Eng.* **2020**, *23*, 414–424. [[CrossRef](#)]
- Chen, W.; Zheng, M. Multi-objective optimization for pavement maintenance and rehabilitation decision-making: A critical review and future directions. *Autom. Constr.* **2021**, *130*, 103840. [[CrossRef](#)]
- Mo T. *JTG 5142-2019; Technical Specifications for Maintenance of Highway Asphalt Pavement*. China Communications Press: Beijing, China, 2019.
- JTG H20-2007; Highway Performance Assessment Standards*. Ministry of Transport of the People's Republic of China: Beijing, China, 2008.
- Anastasopoulos, P.C.; Mannering, F.L. Analysis of Pavement Overlay and Replacement Performance Using Random Parameters Hazard-Based Duration Models. *J. Infrastruct. Syst.* **2015**, *21*, 04014024. [[CrossRef](#)]
- Cinar, Z.M.; Abdussalam Nuhu, A.; Zeeshan, Q.; Korhan, O.; Asmael, M.; Safaei, B. Machine Learning in Predictive Maintenance towards Sustainable Smart Manufacturing in Industry 4.0. *Sustainability* **2020**, *12*, 8211. [[CrossRef](#)]
- Li, F.; Feng, J.; Li, Y.; Zhou, S. *Introduction to the Pavement Preventive Maintenance Technology. Preventive Maintenance Technology for Asphalt Pavement*; Springer Tracts on Transportation and Traffic; Springer: Berlin/Heidelberg, Germany, 2021; pp. 1–35.
- Amarasiri, S.; Muhunthan, B. Evaluating the Effectiveness of Pavement Preventive-Maintenance Treatments in Mitigating Longitudinal Cracks in Wet-Freeze Climatic Zones. *J. Transp. Eng. Part B Pavements* **2020**, *146*, 04020014. [[CrossRef](#)]

14. Yamany, M.S.; Abraham, D.M. Hybrid Approach to Incorporate Preventive Maintenance Effectiveness into Probabilistic Pavement Performance Models. *J. Transp. Eng. Part B Pavements* **2021**, *147*, 04020077. [[CrossRef](#)]
15. Li, J.; Yin, G.; Wang, X.; Yan, W. Automated decision making in highway pavement preventive maintenance based on deep learning. *Autom. Constr.* **2022**, *135*, 104111. [[CrossRef](#)]
16. Hassan, M.U.; Steinnes, O.-M.H.; Gustafsson, E.G.; Løken, S.; Hameed, I.A. Predictive Maintenance of Norwegian Road Network Using Deep Learning Models. *Sensors* **2023**, *23*, 2935. [[CrossRef](#)] [[PubMed](#)]
17. Nautiyal, A.; Sharma, S. Cost-Optimized Approach for Pavement Maintenance Planning of Low Volume Rural Roads: A Case Study in Himalayan Region. *Int. J. Pavement Res. Technol.* **2022**, 1–18. [[CrossRef](#)]
18. Liang, X.; Yu, X.; Chen, C.; Jin, Y.; Huang, J. Automatic Classification of Pavement Distress Using 3D Ground-Penetrating Radar and Deep Convolutional Neural Network. *IEEE Trans. Intell. Transp. Syst.* **2022**, *23*, 22269–22277. [[CrossRef](#)]
19. Xiong, C.; Yu, J.; Zhang, X. Use of NDT systems to investigate pavement reconstruction needs and improve maintenance treatment decision-making. *Int. J. Pavement Eng.* **2021**, 1–15. [[CrossRef](#)]
20. Liu, Z.; Wu, W.; Gu, X.; Li, S.; Wang, L.; Zhang, T. Application of Combining YOLO Models and 3D GPR Images in Road Detection and Maintenance. *Remote Sens.* **2021**, *13*, 1081. [[CrossRef](#)]
21. Hong, X.; Tan, W.; Xiong, C.; Qiu, Z.; Yu, J.; Wang, D.; Wei, X.; Li, W.; Wang, Z. A Fast and Non-Destructive Prediction Model for Remaining Life of Rigid Pavement with or without Asphalt Overlay. *Buildings* **2022**, *12*, 868. [[CrossRef](#)]
22. Di Mascio, P.; Moretti, L. Implementation of a pavement management system for maintenance and rehabilitation of airport surfaces. *Case Stud. Constr. Mater.* **2019**, *11*, e00251. [[CrossRef](#)]
23. Gkyrtis, K.; Plati, C.; Loizos, A. Mechanistic Analysis of Asphalt Pavements in Support of Pavement Preservation Decision-Making. *Infrastructures* **2022**, *7*, 61. [[CrossRef](#)]
24. Nautiyal, A.; Sharma, S. Methods and factors of prioritizing roads for maintenance: A review for sustainable flexible pavement maintenance program. *Innov. Infrastruct. Solut.* **2022**, *7*, 190. [[CrossRef](#)]
25. Elmansouri, O.; Alossta, A.; Badi, I. Pavement Condition Assessment Using Pavement Condition Index and Multi-Criteria Decision-Making Model. *Mechatronics Intell. Transp. Syst.* **2022**, *1*, 57–68. [[CrossRef](#)]
26. Fang, N.; Chang, H.; Hu, S.; Li, H.; Meng, Q. Climate zoning of asphalt pavement based on spatial interpolation and Fuzzy C-Means algorithm. *Int. J. Pavement Eng.* **2022**, 1–14. [[CrossRef](#)]
27. Milad, A.A.; Adwan, I.; Majeed, S.A.; Memon, Z.A.; Bilema, M.; Omar, H.A.; Abdolrasol, M.G.M.; Usman, A.; Yusoff, N.I.M. Development of a Hybrid Machine Learning Model for Asphalt Pavement Temperature Prediction. *IEEE Access* **2021**, *9*, 158041–158056. [[CrossRef](#)]
28. Han, C.; Ma, T.; Chen, S. Asphalt pavement maintenance plans intelligent decision model based on reinforcement learning algorithm. *Constr. Build. Mater.* **2021**, *299*, 124278. [[CrossRef](#)]
29. Ezugwu, A.E.; Ikotun, A.M.; Oyelade, O.O.; Abualigah, L.; Agushaka, J.O.; Eke, C.I.; Akinyelu, A.A. A comprehensive survey of clustering algorithms: State-of-the-art machine learning applications, taxonomy, challenges, and future research prospects. *Eng. Appl. Artif. Intell.* **2022**, *110*, 104743. [[CrossRef](#)]
30. Dalmaijer, E.S.; Nord, C.L.; Astle, D.E. Statistical power for cluster analysis. *BMC Bioinform.* **2022**, *23*, 205. [[CrossRef](#)] [[PubMed](#)]
31. Li, T.; Rezaeipanah, A.; El Din, E.M.T. An ensemble agglomerative hierarchical clustering algorithm based on clusters clustering technique and the novel similarity measurement. *J. King Saud Univ.-Comput. Inf. Sci.* **2022**, *34*, 3828–3842. [[CrossRef](#)]
32. Habib, A.; Akram, M.; Kahraman, C. Minimum spanning tree hierarchical clustering algorithm: A new Pythagorean fuzzy similarity measure for the analysis of functional brain networks. *Expert Syst. Appl.* **2022**, *201*, 117016. [[CrossRef](#)]
33. Ashari, I.F.; Banjarnahor, R.; Farida, D.R.; Aisyah, S.P.; Dewi, A.P.; Humaya, N. Application of Data Mining with the K-Means Clustering Method and Davies Bouldin Index for Grouping IMDB Movies. *J. Appl. Inform. Comput.* **2022**, *6*, 7–15. [[CrossRef](#)]
34. Nie, F.; Li, Z.; Wang, R.; Li, X. An Effective and Efficient Algorithm for K-Means Clustering with New Formulation. *IEEE Trans. Knowl. Data Eng.* **2022**, *35*, 3433–3443. [[CrossRef](#)]
35. Xia, J.; Ying, H.; Huang, Y. Application of ordered aggregation optimal partition method in pavement condition evaluation. In *Frontier Research: Road and Traffic Engineering*; CRC Press: Boca Raton, FL, USA, 2022; pp. 700–706.
36. Tang, H.; Wang, Y.; Jia, K. Unsupervised domain adaptation via distilled discriminative clustering. *Pattern Recognit.* **2022**, *127*, 108638. [[CrossRef](#)]
37. *JTG E60-2008*; Field Test Methods of Highway Subgrade and Pavement. Ministry of Transport of the People’s Republic of China: Beijing, China, 2008.
38. Liu, Z.; Gu, X.; Chen, J.; Wang, D.; Chen, Y.; Wang, L. Automatic recognition of pavement cracks from combined GPR B-scan and C-scan images using multiscale feature fusion deep neural networks. *Autom. Constr.* **2023**, *146*, 104698. [[CrossRef](#)]
39. Wang, S.; Leng, Z.; Sui, X. Detectability of concealed cracks in the asphalt pavement layer using air-coupled ground-penetrating radar. *Measurement* **2023**, *208*, 112427. [[CrossRef](#)]
40. Liu, Z.; Gu, X. Performance evaluation of full-scale accelerated pavement using NDT and laboratory tests: A case study in Jiangsu, China. *Case Stud. Constr. Mater.* **2023**, *18*, e02083. [[CrossRef](#)]
41. Xiong, C.; Yu, J.; Zhang, X.; Korolev, E.; Svetlana, S.; Chen, B.; Chen, F.; Yang, E. Modulus backcalculation methodology based on full-scale testing road and its rationality and feasibility analysis. *Int. J. Pavement Eng.* **2022**, 1–13. [[CrossRef](#)]

42. Burstyn, I. Principal component analysis is a powerful instrument in occupational hygiene inquiries. *Ann. Occup. Hyg.* **2004**, *48*, 655–661. [[CrossRef](#)] [[PubMed](#)]
43. Vidal-Alaball, J.; Mateo, G.F.; Domingo, J.L.G.; Gomez, X.M.; Valmaña, G.S.; Ruiz-Comellas, A.; Seguí, F.L.; Cuyàs, F.G. Validation of a Short Questionnaire to Assess Healthcare Professionals' Perceptions of Asynchronous Telemedicine Services: The Catalan Version of the Health Optimum Telemedicine Acceptance Questionnaire. *Int. J. Environ. Res. Public Health* **2020**, *17*, 2202. [[CrossRef](#)]

Disclaimer/Publisher's Note: The statements, opinions and data contained in all publications are solely those of the individual author(s) and contributor(s) and not of MDPI and/or the editor(s). MDPI and/or the editor(s) disclaim responsibility for any injury to people or property resulting from any ideas, methods, instructions or products referred to in the content.